

<https://doi.org/10.1038/s44298-025-00141-w>

# Detection of avian influenza virus in surface waters using passive samplers

**Madison T. Gouthro, Emalie K. Hayes✉, Taylor Prest & Graham A. Gagnon**

Avian influenza (AIV) remains a global concern not only for humans as a pandemic threat but pose a risk to poultry, wildlife, and livestock. The detection of AIV in the environment traditionally has relied on reactive surveillance, limiting proactive response. This study assessed the detection of Pan-influenza A virus (Pan-FluA) and hemagglutinin subtype H5 genes in surface water using novel passive samplers and molecular analyses. Pan-FluA RNA was detected at concentrations from  $2.1 \times 10^5$  to  $5.6 \times 10^{12}$  copies sampler<sup>-1</sup> and H5 RNA at concentrations from  $2.2 \times 10^4$  to  $1.8 \times 10^{11}$  copies sampler<sup>-1</sup>.

Detections aligned with fall migration and waterfowl activity but also underscored the importance of monitoring interface zones influenced by wildlife, agriculture, and wastewater. Among other hemagglutinin subtypes detected, sequence analyses confirmed the presence of H5 lineages consistent with those reported for H5N1, H5N6, and H5N8. These findings ultimately demonstrate the potential of surface water surveillance as a scalable strategy for AIV detection.

Climate change is intensifying the spread and persistence of waterborne pathogens by altering hydrological and ecological conditions in surface waters. Warmer temperatures can promote pathogen survival and transportation in the environment, while extreme weather events, such as heavy rainfall, hurricanes, and floods, can mobilize animal and human waste into nearby water systems. One of the most well-known examples of climate- and land-use-driven pathogen transmission occurred in Walkerton, Canada, in 2000, when runoff from cattle manure entered a municipal well<sup>1</sup>. Combined with poor chlorination oversight, this resulted in an outbreak of *Escherichia coli* O157:H7 and *Campylobacter* that caused seven deaths and over 2000 illnesses<sup>2</sup>. Notably, a significant proportion of emerging infectious diseases globally are zoonotic, and water is an important transmission medium. As such, there is a need for more surveillance efforts to detect pathogens of concern in aquatic environments like surface water before outbreaks arise.

Avian influenza viruses (AIVs) pose a significant global threat to both wildlife and human health<sup>3</sup>. Wild aquatic birds, particularly waterfowl, serve as primary AIV reservoirs, and to date, 16 hemagglutinin (HA) and 9 neuraminidase (NA) subtypes have been identified in these hosts<sup>4–6</sup>. Most AIVs are classified based on their pathogenicity in birds as either low or high pathogenicity AIV<sup>7</sup>. High pathogenicity AIV is particularly concerning due to its high mortality rate and rapid transmission in poultry, leading to mass die-offs and economic disruption. Subtypes H5 and H7 have been responsible for low and high pathogenicity AIV outbreaks in domestic birds and cattle, but only a limited number of human infections have been reported to date<sup>8</sup>. H5N1 was first detected in North America in 2014 following the introduction of Eurasian-origin AIVs, but has since evolved into

multiple phylogenetic lineages across the world, including clades 2.3.2 and 2.3.4, which have been associated with sporadic transmission to mammals<sup>9–11</sup>. While low pathogenicity AIV strains typically cause mild infections, they remain a surveillance priority because of their potential to spontaneously mutate into high pathogenicity AIV strains<sup>12</sup>.

High pathogenicity AIV surveillance in wild bird populations is largely reactive, often triggered by carcass reports<sup>13</sup>. In Canada, monitoring efforts led by the Canadian Food Inspection Agency (CFIA) include wild bird surveys and domestic poultry surveillance<sup>9,14</sup>. Molecular techniques, particularly reverse transcription polymerase chain reaction (RT-PCR)-based assays that target the FluA matrix, HA, and NA genes, are widely used for AIV detection<sup>12,15–17</sup>. Whole genome sequencing has also been used to trace AIV origins and phylogeny in wildlife and environmental contexts<sup>13</sup>.

Waterfowl, one of the main natural reservoirs for AIVs, are estimated to spend ~15% to 22% of their time in surface waters<sup>18</sup>, shedding virions into these environments through both fecal and oral excretions, which contribute to transmission via the fecal-oral route<sup>16,19</sup>. Consequently, surface water surveillance presents a promising, non-invasive alternative to traditional reactive AIV reporting methods, which typically rely on live bird capture, hunter-submitted specimens, or sporadic carcass identification. However, previous surface water surveillance of AIV has relied on grab sampling<sup>20</sup>, which may lack the sensitivity needed to detect dilute viral signals in large, heterogeneous water bodies<sup>21</sup>. To overcome these limitations, interest in passive sampling for the detection of viruses in water has grown, with studies since 2020 highlighting its advantages over conventional grab and active sampling methods in wastewater and freshwater applications<sup>22,23</sup>. This study, therefore, aimed to evaluate the feasibility of

granular activated carbon (GAC)-based passive sampling, coupled with duplex RT-qPCR and targeted enrichment sequencing, for detecting AIV in surface water lakes and rivers.

## Results

### Detection of avian influenza in Nova Scotia surface waters

Between June and October 2024, 96 GAC-based passive samplers were deployed across five surface water sampling sites in Nova Scotia. Quantitative data were obtained for both the Pan-FluA matrix gene and the H5 HA gene targets (Fig. 1). The Pan-FluA concentrations ranged from  $2.1 \times 10^5$  to  $5.6 \times 10^{12}$  GC sampler $^{-1}$  across all sampling sites, while H5 concentrations ranged from  $2.2 \times 10^4$  to  $1.8 \times 10^{11}$  GC sampler $^{-1}$ . The largest Pan-FluA concentrations were observed at Site 3 ( $\sim 5.6 \times 10^{12}$  GC sampler $^{-1}$ ), whereas Site 5 had the largest H5 concentration ( $\sim 1.8 \times 10^{11}$  GC sampler $^{-1}$ ) (Supplementary Table 1).

Spatial comparisons revealed significant differences in Pan-FluA concentrations between several sites, specifically between Site 2 and Site 4 ( $p = 0.0004$ ), Site 2 and Site 5 ( $p = 0.028$ ), and Site 3 and Site 4 ( $p = 0.005$ ). However, H5 concentrations did not exhibit significant pairwise differences ( $p > 0.05$ ), suggesting a more sporadic spatial distribution. Additionally, within-site comparisons indicated significantly higher Pan-FluA levels than H5 at Site 1 ( $p = 0.021$ ) and Site 4 ( $p = 0.005$ ), but not at the other three sites. Temporal trends showed that Pan-FluA concentrations fluctuated significantly over time at Site 4 ( $p = 0.011$ ); however, H5 remained sporadic and showed no significant temporal variation ( $p > 0.05$ ). These trends contrast with detection-based results, which showed significantly higher detection frequencies of both Pan-FluA and H5 in samples collected from September to October compared to June to August ( $p < 0.05$ ). Site 1 had the highest detection frequency of Pan-FluA (52%), followed by Site 5 (37%), Site 4 (32%), Site 3 (22%), and Site 2 (21%). Conversely, Site 5 had the highest detection frequency of H5 (21%), followed by Site 4 (14%), Site 1 (13%), Site 3 (11%), and Site 2 (5%).

Site-specific waterfowl observations throughout the sampling period further contextualize these findings (Supplementary Fig. 1). Site 3 had the highest and most frequent waterfowl counts, while Sites 1 and 5 were characterized by lower waterfowl counts overall, although both sites exhibited waterfowl present on nearly all days sampled. In comparison, waterfowl were observed at Site 2 only during four sampling events, though with high counts ( $\geq 15$ ) during these sampling events.

Targeted enrichment sequencing was broadly consistent with RT-qPCR results and provided additional resolution on the diversity of Pan-FluA subtypes present in surface water samples (Supplementary Fig. 2). Mean read counts aligned to Pan-FluA reference genomes varied across Sites 1, 3, and 4. Sequence reads aligned to HA and NA segments corresponding to H1, H3, H5, and N1 subtypes at each site. Reads aligned to H5 gene segments with high sequence similarity to reference strains of H5N1, H5N6, and H5N8 viruses. Alignments were most abundant in the matrix and hemagglutinin genes, with inconsistent recovery of complete genome coverage across all eight segments. While multiple Influenza A gene segments were detected, we acknowledge that due to the segmented nature of the genome, sequences cannot be conclusively linked to specific HA-NA subtype pairings.

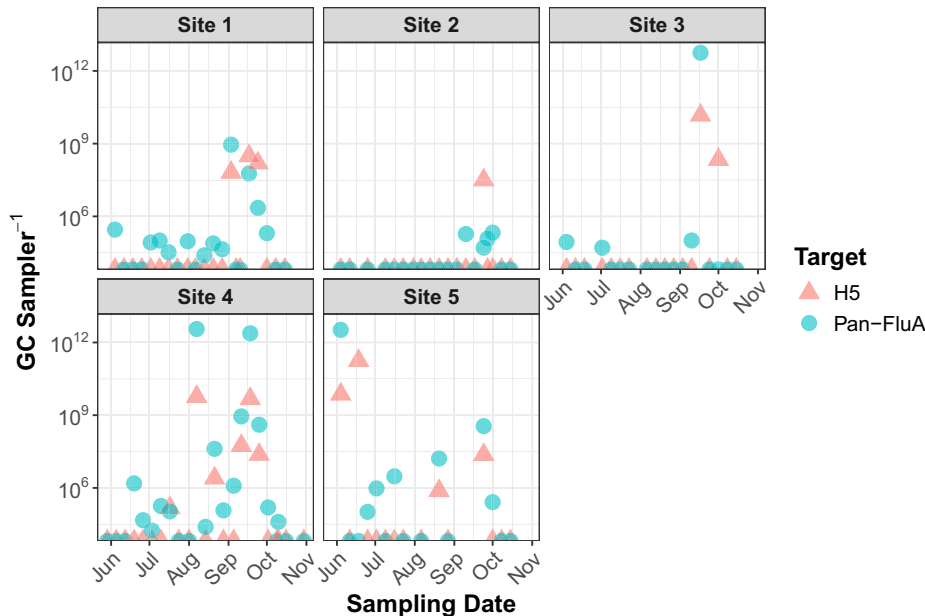
### Site-specific patterns of Pan-FluA, H5, and PMMoV RNA in a freshwater river

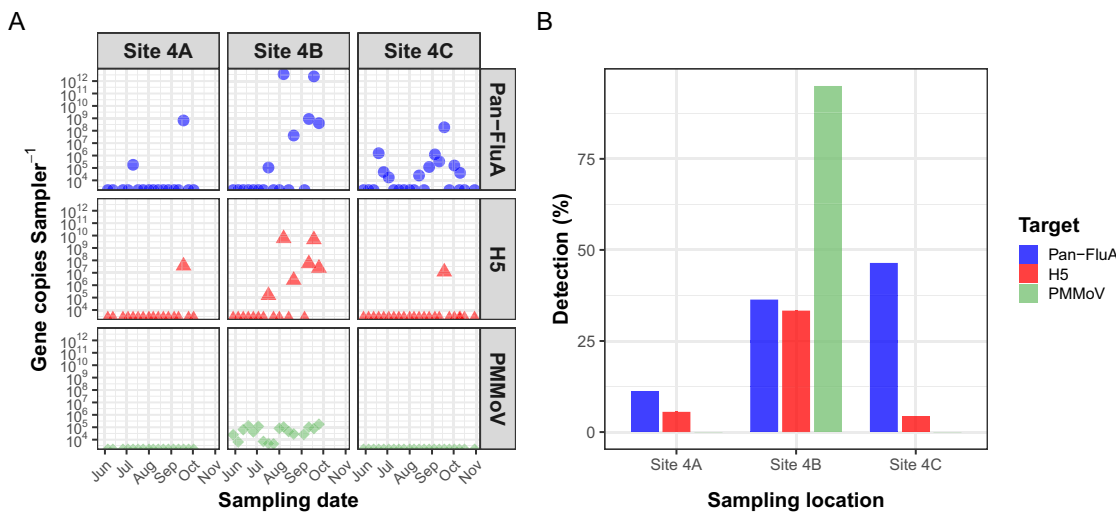
From June to October 2024, 56 GAC-based passive samplers were deployed across three locations (Sites 4A, 4B, and 4C) to evaluate the detection of Pan-FluA, H5, and Pepper Mild Mottle Virus (PMMoV) using RT-qPCR. Site 4A is located at the intake of the municipal drinking water treatment facility, while Site 4B is positioned downstream of Site 4A ( $\sim 1$  km) at the discharge point of the municipal wastewater treatment facility. Site 4C lies further downstream of Site 4B ( $\sim 11$  km) and serves as a designated recreational area for nearby communities. The river stretch between Sites 4B and 4C is surrounded by agricultural land and frequent wildlife activity, both of which were expected to regularly influence viral transport and persistence in the watershed. Additional geographic and land use descriptions for Site 4 are provided in Supplementary Fig. 3, and an overview of the water chemistry across sites is provided in Supplementary Table 2.

Figure 2A illustrates the gene copies (GC) measured across all Site 4 samples collected. Sites 4A, 4B and 4C saw Pan-FluA concentrations ranging from  $1.8 \times 10^5$  to  $6.7 \times 10^8$  GC Sampler $^{-1}$ ,  $6.0 \times 10^4$  to  $3.6 \times 10^{12}$  GC Sampler $^{-1}$  and  $1.7 \times 10^4$  to  $1.9 \times 10^8$  GC Sampler $^{-1}$ , respectively. At Sites 4A and 4C, H5 was only detected in a single sample, with maximum concentrations of  $3.6 \times 10^7$  GC Sampler $^{-1}$  and  $1.2 \times 10^7$  GC Sampler $^{-1}$ , respectively. In contrast, Site 4B detected H5 concentrations from  $2.2 \times 10^4$  to  $4.8 \times 10^9$  GC Sampler $^{-1}$ , while PMMoV was only detected at concentrations ranging from  $2.6 \times 10^3$  to  $1.7 \times 10^5$  GC Sampler $^{-1}$  at Site 4B.

Detection patterns varied across sites and targets (Fig. 2B), with Site 4A exhibiting  $\sim 12\%$  detection frequency of Pan-FluA,  $\sim 6\%$  detection frequency

**Fig. 1 | Temporal detection of Pan-FluA and H5 genes in surface waters using GAC-based passive samplers.** Weekly passive samples were collected from June to October 2024 across five surface water sites in Nova Scotia, Canada, and analyzed using a multiplex RT-qPCR. Samples were processed using a previously validated passive sampling workflow targeting viral adsorption to granular activated carbon. Each panel shows gene copy (GC) concentrations per sampler for Pan-FluA (circles) and H5 (triangles) targets on a log<sub>10</sub> scale for each sampling location. Non-detects for both targets are shown at the bottom of each plot.





**Fig. 2 | Abundance and detection frequencies of Pan-FluA, H5, and PMMoV viral genes in passive samples collected from a freshwater river.** A displays gene copy (GC) concentrations per sampler for Pan-influenza A virus (Pan-FluA), influenza A virus hemagglutinin subtype H5, and Pepper Mild Mottle virus (PMMoV) at three sampling locations within a freshwater river (Sites 4A, 4B, and 4C) in Nova Scotia, Canada measured via RT-qPCR. Blue circles, red triangles, and green squares represent Pan-FluA, H5, and PMMoV detections, respectively. Site 4A is a drinking

water intake, Site 4B is located downstream of wastewater effluent discharge, and Site 4C is a recreational water access point. GC values are plotted on a log<sub>10</sub> scale. B summarizes detection frequency (percentage of positive detections from the total number of samples analyzed) for each viral target at each sampling site. Bars are grouped by site and colored by target: blue for Pan-FluA, red for H5, and green for PMMoV.

of H5, and no PMMoV detections. Site 4B exhibited ~37% detection of Pan-FluA, the highest detection frequencies for H5 (~35%) and PMMoV (100%), coinciding with the strong influence of human and agricultural sources at this site. Site 4C showed the highest Pan-FluA detection frequency (~43%), though H5 was rarely detected (~4%), and PMMoV was not detected in this data set.

## Discussion

The H5 and Pan-FluA detection patterns in this study highlight the ability to capture Pan-FluA and H5 RNA signals in surface waters using passive samplers. The Pan-FluA matrix gene, being highly conserved across Pan-FluA strains, was consistently detected at higher frequencies and concentrations than the H5 gene, which is more genetically diverse and subject to subtype-specific variation<sup>24–26</sup>. The use of the matrix gene ensures broad subtype detection, while the H5-targeted HA gene allows for high-level subtype differentiation<sup>27,28</sup>. This divergence likely reflects the broader circulation and persistence of Pan-FluA in surface waters compared to H5, as well as potential limitations in assay sensitivity for divergent H5 subtypes. Given that the Pan-FluA assay may detect RNA from a range of avian subtypes beyond H5, co-detection of other non-H5 subtypes is possible and warrants further investigation. The RT-qPCR assays used target gene regions conserved across both low- and high-pathogenicity strains and therefore, cannot specify pathogenic potential directly.

Temporal trends revealed elevated Pan-FluA and H5 RNA detections during September and October, which coincide with peak migration along the Atlantic Flyway and correspond to increased avian density at stopover sites, elevating shedding rates<sup>29,30</sup>. Previous studies have shown AIVs to remain infectious for over 200 days in low-salinity waters at 4 °C<sup>29,30</sup>. Cooler water temperatures were measured across sampling sites in October (~13 °C to ~16 °C) compared to warmer water temperatures (>17 °C) in June through September (Supplementary Table 3). As such, the fall season may be an important window for surveillance of influenza viruses. Additionally, spatial variation in Pan-FluA RNA concentrations appeared to be associated with land use surrounding the sampling sites. For example, Sites 4 and 5, located in urbanized and recreational areas, showed elevated Pan-FluA RNA levels, consistent with known influences from wastewater effluent, stormwater runoff, and wildlife activity nearby these sites. Despite similar effluent exposure and recreational use at Site 2, the comparatively lower

Pan-FluA detections suggest that differences in viral contributions or unmeasured site-specific conditions affecting persistence may have contributed to reduced detections at this site. In contrast, consistently high Pan-FluA RNA concentrations at Site 3, where the highest waterfowl presence was observed, support avian fecal shedding as a primary source of viral input. This aligns with a recent systematic review that reported Influenza A concentrations upwards of  $2.5 \times 10^{10}$  copies L<sup>-1</sup> in surface waters frequented by waterfowl<sup>31</sup>. While we were unable to collect concurrent fecal or avian outbreak data in the present study, the consistent Pan-FluA and H5 RNA signals, paired with high waterfowl presence, suggest environmental input was likely through avian shedding. However, paired fecal sampling or environmental viability assessments are required to more definitively link these detections to active infection or transmission. Site 4, where no waterfowl were observed during any sampling events, may have received viral contributions from non-avian sources such as anthropogenic runoff or other wildlife. This is consistent with previous work demonstrating that surface waters influenced by agriculture, livestock operations, and urban runoff can serve as reservoirs for viral contaminants<sup>32</sup>. Overall, the viral concentrations observed in the present study using GAC-based passive samplers are consistent with our previous work, which has observed the detection of respiratory and enteric viruses in a freshwater lake at levels upwards of  $3.9 \times 10^8$  copies per sampler<sup>21</sup>.

This spatial variability was further contextualized by the sub-site analysis at Site 4, which provides a more detailed view of Pan-FluA, H5, and PMMoV RNA signals across different land-use zones within a single watershed. Sampling at the municipal drinking water intake (Site 4A), the wastewater effluent discharge point (Site 4B), and the downstream recreational area (Site 4C) offered insight into how anthropogenic inputs can shape contamination patterns. The low detection frequencies of Pan-FluA and H5 RNA at Site 4A offer some reassurance for source water protection. To further interpret these patterns, PMMoV, a human-associated fecal indicator virus, was monitored alongside Pan-FluA to assist in differentiating between human and non-human sources of contamination along the watershed. PMMoV was detected only at Site 4B, located adjacent to the municipal effluent discharge, and was absent at both the upstream intake (Site 4A) and the downstream recreational location (Site 4C). Indeed, monitoring both PMMoV and Pan-FluA RNA in source waters may provide complementary insights into viral contamination sources. However,

the differences in viral structure, survival, and persistence under dynamic source water conditions must be carefully considered when interpreting results.

Sequencing results further corroborated RT-qPCR findings, offering additional insight into the genomic diversity of Pan-FluA subtypes present in the surface waters monitored. Among other hemagglutinin subtypes detected, sequence analyses confirmed the presence of H5 lineages consistent with those reported for H5N1, H5N6, and H5N8. These detections are supported by regional CFIA reports that confirmed 129 cases of H5N1 and 52 cases of H5N5 in Nova Scotia wildlife between 2022 and early 2025<sup>33</sup>, with ~39% of cases occurring within a ~5500 km<sup>2</sup> area overlapping our sampling sites. While limited sequence coverage precluded definitive source attribution, alignments to H1 and H3 segments were partial and did not allow confident differentiation between human, porcine, or avian lineages. However, the absence of concurrent human H3 outbreaks in the region during the study period and the frequent detection of avian H3N8 in North American wild bird populations suggests a likely avian source<sup>34</sup>. These findings underscore both the advantages and limitations of surface water surveillance, as this approach provides a unique opportunity to detect multiple viral lineages circulating in these environmental reservoirs, but further validation would be required to confirm subtype combinations and pathogenic potential. Further, distinguishing host sources, particularly between zoonotic and anthropogenic inputs, remains a challenge without supporting epidemiological context.

Laboratory studies have demonstrated that AIV can remain infectious at low titers (0.1 TCID<sub>50</sub> mL<sup>-1</sup>) and persist in surface waters under favorable conditions for at least 13 days<sup>35</sup>. While zoonotic transmission through drinking water remains hypothetical, the possibility of cross-species spillover, especially in regions where wastewater infrastructure is inadequate or compromised, warrants consideration. Lucio-Forster et al.<sup>36</sup> proposed that under scenarios of efficient human-to-human transmission of high pathogenicity AIV, domestic wastewater and drinking water systems could serve as pathways for further dissemination of the virus<sup>36</sup>. Furthermore, precipitation-driven sewer overflows have been shown to increase viral loads in surface waters used for potable supply, impacting downstream water quality<sup>37</sup>. In the absence of regulatory thresholds for zoonotic viruses in Canadian drinking water guidelines, surveillance of vulnerable interface zones is warranted. While current Health Canada guidance recommends a 4-log (99.99%) removal/inactivation for enteric viruses using a multi-barrier approach, it does not explicitly address zoonotic pathogens<sup>38,39</sup>. Though laboratory studies have shown that ultraviolet light and chlorine are effective at disinfecting influenza viruses, inactivation dose responses in complex matrices remain poorly characterized<sup>36,40,41</sup>. Consequently, while the risk to municipally treated systems remains low, smaller systems relying on decentralized or private sources may be more vulnerable due to inconsistent treatment or oversight.

The GAC-based passive samplers used in the current study demonstrated consistent performance across the surface water locations sampled, reinforcing their utility for accessible and scalable viral surveillance. Based on our team's field experience gained in this study, we recommend the following: (i) limiting sampler deployments to one-week intervals to optimize signal retention while minimizing nucleic acid degradation; (ii) ensuring samplers are fully submerged and suspended in the water column to avoid interference from turbulence or sediment at the bottom of the water column; and (iii) where feasible, deploy samplers at two to three sites within a watershed to capture spatial variability.

Despite the practical advantages and consistent performance of GAC-based passive samplers observed in this study, several limitations should be noted. We acknowledge that virus recovery is influenced by flow dynamics, organic load, and sampler configuration, which were not directly assessed in this study. The lack of in situ calibration or recovery efficiency measurements also remains a key limitation for quantitative interpretation of passive samplers. Future work could work to address this gap through controlled experiments, such as, establishing recovery efficiencies across realistic gradients of flow, turbidity, temperature, and organic load, would enable more

accurate comparisons across site-specific viral inputs and sampler performance.

In conclusion, the findings presented in this work reinforce the potential value of surface water surveillance as a complementary tool to traditional wildlife-based monitoring of AIV. However, to advance the utility of surface water for surveilling zoonotic disease, greater coordination and data integration are urgently needed across jurisdictional boundaries. Avian hosts and viruses traverse watersheds that span municipal, provincial, and national borders, yet surveillance efforts remain siloed by region and sector. Achieving long-term success in surface water-based monitoring will require integrated frameworks that reflect the ecological realities of trans-boundary viral movement. Effective collaboration among engineers, environmental scientists, wildlife biologists, and public health professionals is critical to align monitoring protocols, facilitate data sharing, and enable timely responses to emerging threats. Although the recent adoption of One Health principles in disease surveillance programs is encouraging, sustained commitment is needed to bridge gaps in knowledge exchange.

## Methods

### Sample collection

Passive samplers were deployed at nine locations across five sites in Nova Scotia, Canada, including four freshwater lakes (Sites 1, 2, 3, and 5) and one river system (Site 4). Sites 2 and 3 each comprised a single sampling location, while Sites 1 and 5 reflect data from two sampling locations per site. Site 4 consisted of three separate locations sampled along the river, representing upstream, midstream, and downstream points in the watershed. Each of the sites had a range of land-use settings, including urban watersheds surrounded by residential and commercial development, some with recreational amenities (e.g., day camps, rowing clubs, walking trails) and adjacent to stormwater outfalls, septic systems, or treated wastewater effluent. Samples were collected weekly from June to October 2024. Passive samplers were deployed at each site and secured using nylon rope, and the rope was either secured to trees along the shoreline or to floating docks. Samplers positioned along the shoreline were placed ~3 m from the water's edge at a depth of ~1 to 2 m below the surface. Samplers deployed from floating docks were suspended ~1.5 m below the water's surface. Sampling was conducted using a GAC-based passive approach, as described in previous research<sup>21</sup>. Each deployment involved deploying ~3 g of GAC in a nylon mesh sleeve with ~25-μm pores, which was then inserted into a passive sampler. A fresh GAC pouch was deployed weekly. After collection, all samples were stored in coolers with ice and transported to the lab immediately upon retrieval of all samples, where they were refrigerated at 4 °C until subsequent analysis.

To assess waterfowl activity at each sampling site, field personnel conducted brief visual counts during each passive sampler retrieval, recording the number of waterfowl observed within a 50-m radius in the water and along the adjacent shoreline. Observations occurred only on a weekly basis during sampler deployments and were carried out during daylight hours. Waterfowl counts were recorded using grouped categories (0, 1–5, 6–10, 11–15, 16–20, 21–25, 26–30) to reduce variability associated with waterfowl movement and visual obstructions. For analysis and visualization, these categories were converted to numeric midpoints to enable site-level comparisons. We acknowledge that these observations do not capture daily variation and may underestimate waterfowl activity between site visits; however, they do offer a broad assessment of the relative waterfowl presence across sites and over time.

### Sample processing methods

Viral RNA was eluted from GAC using an adapted elution protocol based on Hayes et al.<sup>42,43</sup>. Initially, the GAC was removed from the passive sampler and eluted with 40 mL of a buffered solution made up of 0.075% Tween20® +25-mM Tris HCl (sourced from Sigma-Aldrich, Ottawa, ON)<sup>43,44</sup>. To facilitate virus desorption, the mixture was vigorously agitated by vertically inverting the tube ~75 times over ~30 s at ~2.5 inversions per second, before being incubated at room temperature for 1 min<sup>44</sup>. The resulting eluate

was then transferred into a sterile conical tube and stored at 4 °C while awaiting total nucleic acid extraction.

### Total nucleic acid extraction

Following the Promega Wizard® Enviro Total Nucleic Acid Kit protocol, nucleic acids were isolated by first adding a protease solution to each 40 mL sample and incubating for 30 min. The samples were then centrifuged, and 20 mL of the resulting supernatant was transferred into a sterile tube for extraction. Next, binding buffers and isopropanol were added before the mixture was vacuum filtered through a binding column. After washing the column, nucleic acids were eluted into a microcentrifuge tube using 1 mL of nuclease-free water pre-heated to 60 °C. The eluted nucleic acids were then stored at -80 °C until further analysis.

### RT-qPCR

RT-qPCR analysis was carried out on a GeneCount® Q-96 instrument (LuminUltra Technologies Ltd, NB, CA). The duplex RT-qPCR assay targeted the Pan-influenza A virus (Pan-FluA) and hemagglutinin subtype H5 genes<sup>27,45</sup>. Oligonucleotide sequences for the duplex assay were purchased from Integrated DNA Technologies (IA, USA) and are detailed in Supplementary Table 6. Thermal cycling conditions were 55 °C for 10 min, followed by 95 °C for 1 min and then 45 cycles of 95 °C for 10 s and 55 °C for 45 s, and a final hold of 50 °C for 1 min. RT-qPCR reactions were prepared in a total volume of 20 µL using the AgPath-ID™ One-Step RT-PCR Reagents (ThermoFisher, MA, USA). Reactions were prepared with 2X RT-PCR Buffer, 25X RT-PCR Enzyme Mix, and final primer and probe concentrations of 400 nM and 120 nM, respectively.

Human fecal indicator, pepper mild mottle virus (PMMoV) was also quantified using a commercially available RT-qPCR assay from Promega, Corp. (WI, USA). Oligonucleotide sequences for the PMMoV assay are listed in Supplementary Table 6. The PMMoV reactions were prepared following the manufacturer's recommendations, using 15 µL of PCR amplification mix and 5 µL of template. Thermal cycling conditions were carried out as follows: 2 min at 25 °C, 15 min at 50 °C, 2 min at 95 °C, 45 cycles of 15 s at 95 °C, and 30 s at 60 °C.

The performance of the Pan-FluA and H5 duplex assay was validated via measurements of the assay's limit of detection at 95% confidence (LOD<sub>95%</sub>), dynamic quantification range, and reaction efficiency. Standard quantification curves and LOD<sub>95%</sub> determination were carried out using synthetic cDNA fragments (gBlocks®, IDT, IA, USA) and RNA reference material from Twist Bioscience (CA, USA), respectively. The cDNA fragments corresponded to the M1 and HA genes, while the RNA reference material included the HA and NA genes, all from the H5N1 subtype (Supplementary Table 4). The efficiency of the RT-qPCR assay to detect each target was calculated from the slope of the standard quantification curve across a serial dilution of cDNA standard (10<sup>9</sup> to 10<sup>3</sup> copies µL<sup>-1</sup>) using the formula, efficiency = 10<sup>(-1/slope)</sup> - 1 (Supplementary Table 5)<sup>46</sup>. The LOD<sub>95%</sub> values were determined using a logistic regression model, where the proportion of replicates yielding positive amplification was plotted against the concentration of each standard (Supplementary Fig. 4)<sup>47</sup>.

For both RT-qPCR assays, quantitative results were determined using a cycle quantification (Cq) threshold of  $\leq 37$  cycles, with any results above this threshold considered non-detectable. Throughout this work, the standards outlined in the minimum information for publication of qPCR experiments guidelines and environmental microbiology minimum information were followed (Supplementary Table 7)<sup>46,48</sup>. This included carrying out nucleic acid extraction and RT-qPCR preparation in a Thermo Scientific 1300 Series A2 biosafety cabinet (OH, USA) and a Mystaire MY Model PCR Prep Station Class 100 laminar flow enclosure, respectively. Field blanks collected during each sampling day were processed in parallel with test samples. All RT-qPCR runs had at least one negative template control included, and any observed amplification from a negative control resulted in the exclusion and repetition of the entire run. If a test sample had one undetected replicate, it was re-analyzed at 1:5 and 1:10 dilutions using nuclease-free water to account for potential PCR inhibition. For the preparation of calibration

curves, synthetic standards were prepared in single-use aliquots and handled in a separate workspace with dedicated pipettes and aerosol-resistant filter tips to further reduce the risk of contamination. No amplification was observed in field blanks or NTCs throughout the study.

### Targeted enrichment sequencing

Targeted enrichment sequencing was conducted to confirm the presence and identity of H5 lineages in samples that tested positive by RT-qPCR. Sequencing was conducted on all nucleic acid extracts using the Illumina Viral Surveillance Panel Kit v2 (Illumina, Inc., CA, USA), which comprises reference genomes for over 200 viruses and subtypes. Library preparation followed the Illumina RNA prep with enrichment protocol utilizing bead-linked transposomes technology paired with fast enrichment. In brief, 8.5 µL of total nucleic acid extract was denatured before undergoing first- and second-strand DNA synthesis, followed by cDNA fragmentation. The resulting DNA fragments were subsequently purified and amplified to integrate index adapter sequences for dual indexing. This study utilized index set A from the four available Illumina index sets (A, B, C, and D), each containing 96 unique single-use DNA/RNA UD indexes. Post-amplification, the libraries were purified and quantified using the Invitrogen Qubit dsDNA Broad Range Assay Kit (Thermo Fisher Scientific, MA, USA) and the Agilent TapeStation H5 D1000 (BW, Germany). A 7.5 µL aliquot from each library was hybridized with oligonucleotides from the Illumina viral panel, followed by bead capture of the hybridized probes. The enriched libraries then underwent PCR amplification, further purification, and final quantification using the Qubit dsDNA Broad Range Assay Kit. Normalization was performed to achieve a concentration of 2 nM, with final dilution to a loading concentration of 600 pM. Sequencing was carried out on the Illumina NextSeq 1000 platform (Illumina, CA, USA) utilizing the P1 XLEAP-SBS™ 300 cycles Kit (2 × 150 bp).

The run metrics were evaluated on the BaseSpace app by analyzing cluster density and Q30 score. Demultiplexing of the raw sequencing data in Illumina's Cloud-based BaseSpace Sequence Hub generated FASTQ files for each sample. Individual FASTQ file format sequencing files were then analyzed using the Illumina DRAGEN™ Microbial enrichment pipeline (v3.5.16) using default parameters to identify specific viral sequence detection and coverage in the samples by comparing the sequence data to the provided reference genomes<sup>49</sup>. A reads per kilobase per million reads threshold of five was applied for data reporting.

### Data analysis

The number of gene copies µL<sup>-1</sup> detected by RT-qPCR was normalized to the total original GAC sampler elution volume to estimate the cumulative gene copies recovered per sampler during the weekly deployments (Eq. 1), following previously established approaches outlined by Hayes et al.<sup>22</sup>. This approach reflects the cumulative genomic copies adsorbed to the passive sampler over a deployment period and are not intended to estimate viability or volumetric concentrations.

$$GC\ Sampler^{-1} = (GC\ \mu L^{-1} \times 1000\ (\mu L)) \times Sampler\ Elution\ Volume(mL) \quad (Eq.1)$$

Data analyses were conducted in RStudio Version (2024.04.2 + 764), using the packages *tidyverse*, *scales*, *lme4*, *mgcv*, *lubridate*, *readxl*, and *emmeans*<sup>50-55</sup>. A generalized additive model was used to assess nonlinear temporal trends and spatial differences in viral detections. Detection frequencies of viral targets were compared using chi-squared analysis, while differences in gene copy concentrations were assessed using a linear mixed-effects model on log-transformed values. Pairwise comparisons of mean values were performed, and statistical significance was determined at  $\alpha = 0.05$ .

### Data availability

The datasets used in the current study are available within the manuscript and the Supplementary Information files. Any additional data supporting

the findings of this study are available from the corresponding author upon request.

## Code availability

No custom code or scripts were used to generate or analyze datasets. Full details of the statistical models and scripts used for figure generation are available in the cited references provided in “Data analysis”. No proprietary or restricted-access software was used.

Received: 28 May 2025; Accepted: 5 July 2025;

Published online: 17 July 2025

## References

1. Hrudey, S. E., Huck, P. M., Payment, P., Gillham, R. W. & Hrudey, E. J. Walkerton: lessons learned in comparison with waterborne outbreaks in the developed world. *J. Environ. Eng. Sci.* **1**, 397–407 (2002).
2. Clark, C. G. et al. Characterization of waterborne outbreak-associated *Campylobacter jejuni*, Walkerton, Ontario. *Emerg. Infect. Dis.* <https://doi.org/10.3201/eid0910.020584> (2003).
3. Renaud, C. et al. Highly pathogenic avian influenza: unprecedented outbreaks in Canadian wildlife and domestic poultry. *J. Assoc. Med. Microbiol. Infect. Dis. Can.* **8**, 187–191 (2023).
4. Sturm-Ramirez, K. M. et al. Reemerging H5N1 influenza viruses in Hong Kong in 2002 are highly pathogenic to ducks. *J. Virol.* **78**, 4892–4901 (2004).
5. CDC. Types of Influenza Viruses. *Influenza (Flu)* <https://www.cdc.gov/flu/about/viruses-types.html> (2024).
6. Kosik, I. & Yewdell, J. W. Influenza hemagglutinin and neuraminidase: Yin-Yang proteins coevolving to thwart immunity. *Viruses* **11**, 346 (2019).
7. Luczo, J. M. & Spackman, E. Molecular evolution of the H5 and H7 highly pathogenic avian influenza virus haemagglutinin cleavage site motif. *Rev. Med. Virol.* **35**, e70012 (2025).
8. CDC. Avian Influenza Type A. *Avian Influenza (Bird Flu)* <https://www.cdc.gov/bird-flu/about/avian-influenza-type-a.html> (2025).
9. Canada, E. & C. C. Avian influenza in wild birds. <https://www.canada.ca/en/environment-climate-change/services/migratory-game-bird-hunting/avian-influenza-wild-birds.html> (2015).
10. Jhung, M. A. & Nelson, D. I. Outbreaks of avian influenza A (H5N2), (H5N8), and (H5N1) among birds—United States, December 2014–January 2015. *Morb. Mortal. Wkly. Rep.* **64**, 111 (2015).
11. Murti, M. et al. Public health response to outbreaks of Avian Influenza A(H5N2) and (H5N1) among poultry—British Columbia, December 2014–February 2015. *Can. Commun. Dis. Rep.* **41**, 69–72 (2015).
12. Widjaja, L., Krauss, S. L., Webby, R. J., Xie, T. & Webster, R. G. Matrix gene of influenza A viruses isolated from wild aquatic birds: ecology and emergence of influenza A viruses. *J. Virol.* **78**, 8771–8779 (2004).
13. Giacinti, J. A. et al. Avian influenza viruses in wild birds in Canada following incursions of highly pathogenic H5N1 virus from Eurasia in 2021–2022. *mBio* **15**, e03203-23 (2024).
14. Parmley, J., Lair, S. & Leighton, F. A. Canada’s inter-agency wild bird influenza survey. *Integr. Zool.* **4**, 409–417 (2009).
15. Laconi, A. et al. Detection of avian influenza virus: a comparative study of the in silico and in vitro performances of current RT-qPCR assays. *Sci. Rep.* **10**, 8441 (2020).
16. Hubbard, L. E. et al. Environmental surveillance and detection of infectious highly pathogenic avian influenza virus in Iowa wetlands. *Environ. Sci. Technol. Lett.* **10**, 1181–1187 (2023).
17. Stone, B. et al. Rapid detection and simultaneous subtype differentiation of influenza A viruses by real-time PCR. *J. Virol. Methods* **117**, 103–112 (2004).
18. Jones, T. A., Waitt, C. D. & Dawkins, M. S. Water off a duck’s back: showers and troughs match ponds for improving duck welfare. *Appl. Anim. Behav. Sci.* **116**, 52–57 (2009).
19. Domanska-Blicharz, K., Minta, Z., Smietanka, K., Marché, S. & van den Berg, T. H5N1 high pathogenicity avian influenza virus survival in different types of water. *Avian Dis* **54**, 734–737 (2010).
20. Ahrens, A. K. et al. Investigating environmental matrices for use in avian influenza virus surveillance—surface water, sediments, and avian fecal samples. *Microbiol. Spectr.* **11**, e02664–22 (2023).
21. Hayes, E. K., Gouthro, M. T., Fuller, M., Redden, D. J. & Gagnon, G. A. Enhanced detection of viruses for improved water safety. *Sci. Rep.* **13**, 17336 (2023).
22. Hayes, E. K. & Gagnon, G. A. From capture to detection: a critical review of passive sampling techniques for pathogen surveillance in water and wastewater. *Water Res.* **122024** <https://doi.org/10.1016/j.watres.2024.122024> (2024).
23. Bivins, A. et al. Passive sampling to scale wastewater surveillance of infectious disease: Lessons learned from COVID-19. *Sci. Total Environ.* **835**, 155347 (2022).
24. Horn, N., Gentles, L., Bloom, J. D. & Lee, K. K. Deep mutational scan of the highly conserved influenza A virus M1 Matrix protein reveals substantial intrinsic mutational tolerance. *J. Virol.* **93**, e00161–19 (2019).
25. Nao, N. et al. A single amino acid in the M1 protein responsible for the different pathogenic potentials of H5N1 highly pathogenic avian influenza virus strains. *PLOS ONE* **10**, e0137989 (2015).
26. Zhu, Y. et al. Molecular patterns of matrix protein 1 (M1): a strong predictor of adaptive evolution in H9N2 avian influenza viruses. *Proc. Natl. Acad. Sci. USA* **122**, e2423983122 (2025).
27. Wolfe, M. K. et al. Detection of hemagglutinin H5 influenza A virus sequence in municipal wastewater solids at wastewater treatment plants with increases in influenza A in spring, 2024. *Environ. Sci. Technol. Lett.* **11**, 526–532 (2024).
28. Spackman, E. et al. Development of a real-time reverse transcriptase PCR assay for type A influenza virus and the avian H5 and H7 hemagglutinin subtypes. *J. Clin. Microbiol.* **40**, 3256–3260 (2002).
29. Dublineau, A. et al. Persistence of the 2009 pandemic influenza A (H1N1) virus in water and on non-porous surface. *PLoS ONE* **6**, e28043 (2011).
30. Ramey, A. M. et al. Evidence for interannual persistence of infectious influenza A viruses in Alaska wetlands. *Sci. Total Environ.* **803**, 150078 (2022).
31. Kenmoe, S. et al. A systematic review of influenza virus in water environments across human, poultry, and wild bird habitats. *Water Res. X* **22**, 100210 (2023).
32. Gilbert, M. et al. Mapping H5N1 highly pathogenic avian influenza risk in Southeast Asia. *Proc. Natl. Acad. Sci. USA* **105**, 4769–4774 (2008).
33. Canadian Food Inspection Agency Government of Canada. National Avian Influenza - Wild Positives. [https://www.cwhc-rcsf.ca/avian\\_influenza.php](https://www.cwhc-rcsf.ca/avian_influenza.php) (2025).
34. Wang, Y. et al. Prevalence, evolution, replication, and transmission of H3N8 avian influenza viruses isolated from migratory birds in eastern China from 2017 to 2021. *Emerg. Microbes Infect.* **12**, 2184178 (2023).
35. Ahrens, A. K., Selinka, H.-C., Mettenleiter, T. C., Beer, M. & Harder, T. C. Exploring surface water as a transmission medium of avian influenza viruses—systematic infection studies in mallards. *Emerg. Microbes Infect.* **11**, 1250–1261 (2022).
36. Lucio-Forster, A., Bowman, D. D., Lucio-Martínez, B., Labare, M. P. & Butkus, M. A. Inactivation of the avian influenza virus (H5N2) in typical domestic wastewater and drinking water treatment systems. <https://home.liebertpub.com/ees>. <https://www.liebertpub.com/doi/10.1089/ees.2006.23.897>. <https://doi.org/10.1089/ees.2006.23.897> (2006).
37. Prevost, B. et al. Large scale survey of enteric viruses in river and waste water underlines the health status of the local population. *Environ. Int.* **79**, 42–50 (2015).

38. Health Canada. *Enteric Viruses In Drinking Water* (Health Canada, 2017).
39. U.S. EPA. *Surface Water Treatment Rules*. <https://www.epa.gov/dwreginfo/surface-water-treatment-rules> (U.S. EPA, 2015).
40. Rice, E. W. et al. Chlorine inactivation of highly pathogenic avian influenza virus (H5N1). *Emerg. Infect. Dis.* **13**, 1568–70 (2007).
41. Lénès, D. et al. Assessment of the removal and inactivation of influenza viruses H5N1 and H1N1 by drinking water treatment. *Water Res.* **44**, 2473–2486 (2010).
42. Hayes, E. K., Stoddart, A. K. & Gagnon, G. A. Adsorption of SARS-CoV-2 onto granular activated carbon (GAC) in wastewater: Implications for improvements in passive sampling. *Sci. Total Environ.* **847**, 157548 (2022).
43. Hayes, K. et al. A novel passive sampling approach for SARS-CoV-2 in wastewater in a Canadian province with low prevalence of COVID-19. *Environ. Sci. Water Res. Technol.* **7**, 1576–1586 (2021).
44. Gouthro, M., Hayes, E. K. & Gagnon, G. A. Maximizing viral nucleic acid yield from passive samplers: evaluating elution and extraction protocols. *Sci. Total Environ.* **957**, 177834 (2024).
45. Sahoo, M. K. et al. Multiplex dual-target reverse transcription PCR for subtyping avian influenza A(H5) virus. *CDC* **30**, 1710–1713 (2024).
46. Bustin, S. A. et al. The MIQE guidelines: minimum information for publication of quantitative real-time PCR experiments. *Clin. Chem.* **55**, 611–622 (2009).
47. Forootan, A. et al. Methods to determine limit of detection and limit of quantification in quantitative real-time PCR (qPCR). *Biomol. Detect. Quantif.* **12**, 1–6 (2017).
48. Borchardt, M. A. et al. The Environmental Microbiology Minimum Information (EMMI) guidelines: qPCR and dPCR quality and reporting for environmental microbiology. *Environ. Sci. Technol.* **55**, 10210–10223 (2021).
49. DRAGEN secondary analysis | Software for NGS data analysis. <https://www.illumina.com/products/by-type/informatics-products/dragen-secondary-analysis.html> (2023).
50. Wickham, H. et al. Welcome to the tidyverse. *J. Open Source Softw.* **4**, 1686 (2019).
51. Wilke, C. O. & Wiernik, B. M. ggtext: improved text rendering support for “ggplot2”. (2022).
52. Wickham, H., Pedersen, T. L. & Seidel, D. Scales: scale functions for visualization. <https://scales.r-lib.org/> (2023).
53. Aphalo, P. J. ggpmisc: Miscellaneous Extensions to ‘ggplot2’. 0.6.1 <https://doi.org/10.32614/CRAN.package.ggpmisc> (2016).
54. Pedersen, T. L. patchwork: The Composer of Plots. 1.3.0 <https://doi.org/10.32614/CRAN.package.patchwork> (2019).
55. Grolemund, G. & Wickham, H. Dates and times made easy with lubridate. *J. Stat. Softw.* **40**, 1–25 (2011).

## Acknowledgements

This study was funded through support from the NSERC Alliance program (ALLRP 568507 - 21) and its member partners, which include LuminUltra Technologies Ltd, Mantech Inc., AGAT Laboratories, Halifax Water, AquiSense Technologies, CBCL Limited, City of Moncton, and Cape Breton Regional Municipality. The authors gratefully acknowledge the contributions

of Halifax Regional Municipality and Dr. Jason Leblanc at Nova Scotia Health, whose partnership and input were integral to the direction and achievement of the project. We would also like to extend thanks to students Emily Niskanen, Esma Abibulaieva, Saksham Bafna, and Christian Lyons from Dalhousie University’s Centre for Water Resources Studies for their laboratory support throughout the study.

## Author contributions

M.G. performed data validation, conducted statistical analyses, and contributed to manuscript writing and revision. E.H. developed the methodology, administered the project, prepared all data visualizations, conducted statistical analyses, and contributed to manuscript writing and revision. T.P. collected and analyzed samples and contributed to manuscript writing and editing. G.G. supervised the project, acquired funding, provided technical oversight, and contributed to manuscript review and editing. All authors contributed to the study’s conception or design, and all authors have read and approved the final version of the manuscript.

## Competing interests

The authors declare no competing interests.

## Additional information

**Supplementary information** The online version contains supplementary material available at <https://doi.org/10.1038/s44298-025-00141-w>.

**Correspondence** and requests for materials should be addressed to Emalie K. Hayes.

**Reprints and permissions information** is available at <http://www.nature.com/reprints>

**Publisher’s note** Springer Nature remains neutral with regard to jurisdictional claims in published maps and institutional affiliations.

**Open Access** This article is licensed under a Creative Commons Attribution-NonCommercial-NoDerivatives 4.0 International License, which permits any non-commercial use, sharing, distribution and reproduction in any medium or format, as long as you give appropriate credit to the original author(s) and the source, provide a link to the Creative Commons licence, and indicate if you modified the licensed material. You do not have permission under this licence to share adapted material derived from this article or parts of it. The images or other third party material in this article are included in the article’s Creative Commons licence, unless indicated otherwise in a credit line to the material. If material is not included in the article’s Creative Commons licence and your intended use is not permitted by statutory regulation or exceeds the permitted use, you will need to obtain permission directly from the copyright holder. To view a copy of this licence, visit <http://creativecommons.org/licenses/by-nc-nd/4.0/>.

© The Author(s) 2025